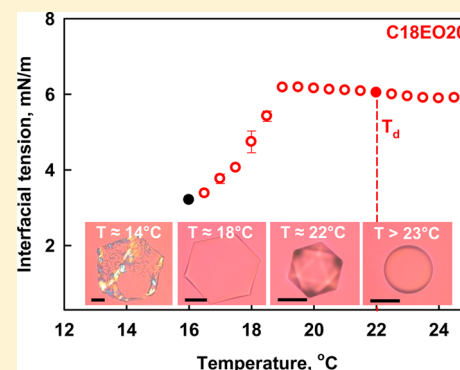


On the Mechanism of Drop Self-Shaping in Cooled Emulsions

Nikolai Denkov,[†] Diana Cholakova,[†] Slavka Tcholakova,[†] and Stoyan K. Smoukov^{*,‡}[†]Department of Chemical and Pharmaceutical Engineering, Faculty of Chemistry and Pharmacy, Sofia University, 1164 Sofia, Bulgaria[‡]Active and Intelligent Materials Lab, Department of Materials Science & Metallurgy, University of Cambridge, Cambridge CB3 0FS, U.K.

Supporting Information

ABSTRACT: Two recent studies (Denkov et al., *Nature* 2015, 528, 392 and Guttman et al. *Proc. Natl. Acad. Sci. U.S.A.* 2016, 113, 493) demonstrated that micrometer-sized *n*-alkane drops, dispersed in aqueous surfactant solutions, can break their spherical symmetry upon cooling and self-shape into a variety of regular shapes, such as fluid polyhedra, platelet-shaped hexagons, triangles, rhomboids, toroids, and submicrometer-diameter fibers. In the first study, the observed phenomenon was explained by a mechanism involving the formation of interfacial multilayer of self-assembled alkane molecules in the so-called rotator phases, templated by the frozen surfactant adsorption layer. Such phases are known to form in alkane droplets under similar conditions and are sufficiently strong to deform the droplets against the capillary pressure of a finite interfacial tension of several mN/m. The authors of the second study proposed a different explanation, namely, that the oil–water interfacial tension becomes ultralow upon cooling, which allows for surface extension and drop deformation at negligible energy penalty. To reveal which of these mechanisms is operative, we measure in the current study the temperature dependence of the interfacial tensions of several systems undergoing such drop-shape transitions. Our results unambiguously show that drop self-shaping is not related to ultralow oil–water interfacial tension, as proposed by Guttman et al. These results support the mechanism proposed by Denkov et al., which implies that the large bending moment, required to deform an oil–water interface with an interfacial tension of 5 to 10 mN/m, is generated by an interfacial multilayer of self-assembled alkane molecules.



INTRODUCTION

In two recent studies,^{1,2} it was shown experimentally that micrometer sized *n*-alkane drops, dispersed in aqueous surfactant solutions, can break symmetry upon cooling and self-shape into a variety of regular forms. This phenomenon is important for two wide research areas because it provides (1) a new, highly efficient bottom-up approach for producing particles with complex shapes and (2) a system, remarkably simple in chemical composition, that exhibits the basic processes of structure and shape transformations, reminiscent of morphogenesis events in living organisms.

This self-shaping phenomenon is far from trivial because it involves a spontaneous deformation of the drop surface in the process of drop cooling, against the capillary pressure that acts to preserve the spherical shape of the drop. Drop deformation rarely happens spontaneously because any deformation of the surface of spherical drops increases the surface area and leads to a concomitant penalty by increasing the drop-surface energy.

To explain their experimental results, the authors of the original papers^{1,2} proposed two alternative mechanisms in their studies. One of the mechanisms^{2,3} assumes that the interfacial tension becomes ultralow upon cooling (and even becomes transiently negative), which allows for surface extension and deformation at minimal or vanishing energy penalty. The alternative mechanism^{1,4} assumes the formation of molecular multilayers of a rotator phase^{5–7} at the drop surface being

templated by the frozen surfactant adsorption layer, which counteracts a finite interfacial tension (rotator phases were previously detected^{8–11} by X-ray and DSC methods in such alkane droplets). As estimated in ref 1, such multilayers with a thickness of several hundred nanometers may have a cumulative bending moment that is sufficiently high to deform an oil–water interface with interfacial tension greater than 5 mN/m.

In more recent studies,^{3,4} the two research groups further elaborated their arguments in defense of their original ideas. Of special interest is ref 4, where it was shown experimentally that the observed phenomenon is not limited to drops of linear *n*-alkanes, as reported in the original papers, but is also observed with several other classes of molecules, such as triglycerides, *n*-alcohols, *n*-alkenes, and alkylcyclohexanes. In this study,⁴ drop self-shaping was observed with more than 60 different surfactant–organic liquid combinations, all of them following the same general evolution path, as described in ref 1. With respect to their effect on drop deformations, the surfactants studied were classified into four distinct groups (denoted as A to D). These results showed that the self-shaping phenomenon is much more general than initially thought.

Received: April 30, 2016

Revised: June 27, 2016

Published: July 18, 2016

To reveal which of the two proposed mechanisms^{1,2} is relevant to this phenomenon, in the current study we measure the temperature dependence of the interfacial tensions of several systems undergoing such drop-shape transitions. One of the systems has the same composition as the single system studied in ref 2. The other systems are taken to represent the four groups of the surfactants, studied in refs 1 and 4. Thus, we cover the entire range of systems shown to exhibit this phenomenon so far.

EXPERIMENTAL SECTION

Materials. We use hexadecane as the organic phase in all of the experiments here because this is the main organic phase studied in refs 1–3. Hexadecane was purified from surface-active contamination by passing through a glass column filled with Florisil adsorbent. It has a melting point of the bulk phase of $T_m = 18$ °C. The interfacial tension of the clean hexadecane–water interface was measured at 25 °C by the pendant drop method, described later in this section. The experimental data shown in Figure S1 (Supporting Information) demonstrate that the interfacial tension stays at 52 ± 0.5 mN/m for a period of as long as 15 min. This result is a clear indication that the hexadecane and water phases used are very pure with respect to surface-active contamination.

As surfactants we used the following water-soluble substances (in parentheses, trade name and company obtained from): nonionic surfactants polyoxyethylene alkyl ether C₁₈EO₂₀ (Brij 78, Sigma-Aldrich), C₁₆EO₂₀ (Brij 58, Sigma-Aldrich), C_{16–18}EO₅₀ (Lutensol AT50, BASF), and polyoxyethylene sorbitan monoalkylate C₁₈SorbEO₂₀ (Tween 60, Sigma-Aldrich). We also used cationic surfactant octadecyltrimethylammonium bromide (C₁₈TAB, TCI Chemicals). The purity of C₁₈TAB was >98%, and the nonionic surfactants were of commercial grade. All surfactants were used without further purification. Information for the surfactant producers and properties is presented in Table S1 in Supporting Information.

All aqueous solutions were prepared with deionized water (with resistivity >18 MΩ·cm), which was purified by an Elix 3 module (Millipore).

Emulsion Preparation. All emulsions were prepared by membrane emulsification in which drops with a relatively narrow size distribution were generated.^{12–15} The hexadecane phase was emulsified by passing it through the membrane pores under pressure into the continuous phase (aqueous surfactant solution). We used a laboratory Microkit membrane emulsification module from Shirasu Porous Glass Technology (SPG, Miyazaki, Japan), working with tubular glass membranes with an outer diameter of 10 mm and a working area of approximately 3 cm². Membranes with a mean pore diameter of 10 μm were used to prepare emulsions with a drop diameter of $\sim 32 \pm 3$ μm. For some of the surfactants, experiments with smaller drops (5, 10, or 15 μm in diameter) were performed.

Optical Observation of the Drop-Shape Transformations. For microscope observations, the emulsions were transferred in glass capillaries with a rectangular cross-section (50 mm length, 1 mm width, and 0.1 mm height) enclosed within a custom-made cooling chamber, with optical windows for microscope observation (Figure 1). The observations were performed with optical microscope Axioplan or AxioImager M.2m (Zeiss, Germany) in transmitted, cross-polarized white light. Long-focus objectives $\times 20$, $\times 50$, and $\times 100$, combined with built-in cross-polarizing accessories of the microscope, were used to observe the drops upon sample cooling. An additional λ plate (compensator plate) was situated between the polarizer and the analyzer, the latter two being oriented at 90° with respect to each other. The λ plate was oriented at 45° with respect to both the polarizer and the analyzer. Under these conditions, the liquid background and the fluid objects have a typical magenta color, whereas the birefringent areas appear brighter and may have intense colors.^{16,17}

The temperature of the cooling chamber was controlled by a cryothermostat (Julabo CF30) and measured close to the emulsion

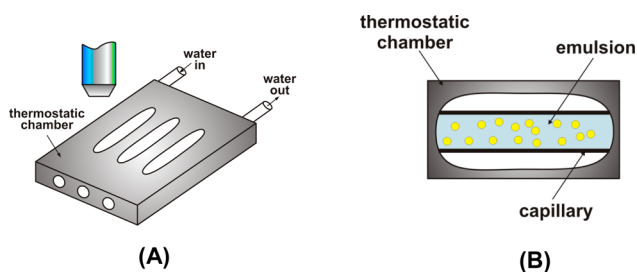


Figure 1. (A) Schematic presentation of the cooling chamber, made of aluminum, with optical windows cut out, used for microscope observation of the emulsion samples. (B) The emulsions studied were contained in glass capillaries, placed in the thermostatic chamber, and observed through the optical windows.

location using a calibrated thermocouple probe with an accuracy of ± 0.2 °C. Experiments were carried out at a cooling rate varied between 0.1 and 1.5 K/min.

We estimate theoretically the time, τ , required to cool an emulsion drop with diameter $d \approx 40$ μm, assuming negligible drop heating due to phase transitions or viscous friction inside the drop (both processes generate heat). The time for the temperature at the drop center to equilibrate to 95% of the temperature difference from the surface is around 5 ms, as shown in eq 1:²⁰

$$\tau \approx \frac{d^2}{4\chi} = \frac{(40 \mu\text{m})^2}{3.2 \times 10^{-7}} = 5 \text{ ms} \quad (1)$$

Here $\chi = (\kappa/\rho C_p)$ is the thermal diffusivity of the dispersed phase, and κ , ρ , and C_p are its thermal conductivity, mass density, and heat capacity, respectively. For planar slabs, to find the time for the temperature in the center to equilibrate to 90% of the difference from the outside, the same equation (eq 1) holds if one replaces the drop diameter with the slab thickness.²⁰ When our particles flatten, their thickness becomes significantly smaller than the initial drop diameter, so the equilibration time is even shorter. Because of the low cooling rates in our experiments and most deformations occurring on time scales of seconds to minutes, we assume that the temperatures of the droplets and of the continuous phase were virtually the same. This assumption does not imply that all observed phenomena are equilibrium ones because some of the drop-shape transformations could take a very long time (e.g., the extrusion of the thin threads from the corners of the deformed drop).

Interfacial Tension. The hexadecane–water interfacial tension, γ , was measured by drop-shape analysis at different temperatures.^{18,19} The shape of millimeter-sized pendant oil drops, immersed in the surfactant solution, was recorded and analyzed by the Laplace equation of capillarity to determine the oil–water interfacial tension (DSA100 instrument by Krüss, Germany). The TC40 thermostating cell was used to vary the temperature of the measured system with a precision of ± 0.2 °C. The time required to cool a drop of millimeter size was estimated to be $\tau \approx 5$ s (eq 1).

In a typical experiment, the temperature was decreased with a rate mimicking that in the actual experiments with slowly cooled emulsions (between 0.1 and 0.5 K/min). In separate experiments, the actual temperature at the position of the pendant drop was measured by a calibrated thermocouple. Also, for some of the systems a discrete set of decreasing temperatures was used, with equilibration of 15 or 60 min at each temperature. For a given temperature, the interfacial tensions measured at a constant cooling rate and at a fixed temperature were in agreement, with the tension measured at constant temperature being the same or only slightly lower (up to 0.5 mN/m) because a very slow rearrangement of the molecules may take place in the frozen adsorption layers. The latter difference was observed at the lowest temperatures only, and the deformation of the emulsified drop in the same solution had already started at higher temperatures.

Because the experiments at a constant cooling rate better mimic the actual experiments with cooled emulsions, we show these data for the interfacial tension in Figures 2–4 and S2–S3.

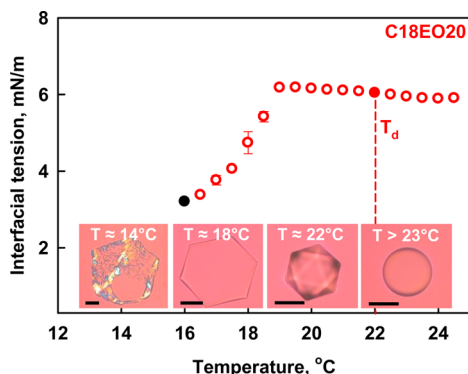


Figure 2. Interfacial tension as a function of temperature for a hexadecane drop, immersed in a 1.5 wt % (13 mM) aqueous solution of nonionic surfactant $C_{18}EO_{20}$, as measured by the pendant drop method. The insets show microscope images of deformed emulsion drops captured at different temperatures. Note that the drop deformation starts at $T_d = 22 \pm 0.5$ °C when the interfacial tension is 6.0 ± 0.2 mN/m. The pendant drop freezes at 16 °C when the interfacial tension is still >3 mN/m, and the emulsified drop takes the shape of a hexagonal platelet at this temperature. Scale bars are $20 \mu\text{m}$.

RESULTS AND DISCUSSION

In Figure 2, we show the experimental data for the interfacial tension of hexadecane drops, immersed in a 1.5 wt % (13 mM) aqueous solution of nonionic surfactant $C_{18}EO_{20}$, which induces drop-shape transformations starting at T_d above the bulk oil melting temperature, $T_d > T_m$ (belonging to surfactant Group A, as defined in ref 4). At 19 ± 0.2 °C, there is a break point in the curve of interfacial tension vs temperature, and the slope changes from negative at higher temperature to positive at lower temperature. The 1 mm pendant drop, cooled at 0.15 K/min, freezes at 16 °C when the interfacial tension is still higher than 3 mN/m; see the solid black circle in the data for the interfacial tension in Figure 2. At this temperature, the emulsified drops have the shape of a hexagonal platelet.

As insets in Figure 2, we show the images of emulsified hexadecane drops with an initial diameter of $31 \pm 2 \mu\text{m}$ in the same surfactant solution. Remarkably, the deformation of the emulsified drops starts at $T_d = 22 \pm 0.5$ °C when the interfacial tension is rather high, 6.0 ± 0.2 mN/m (see the red full circle in the data for the interfacial tension). The emulsified drop acquires the shape of a flat hexagonal platelet at 18 ± 0.5 °C when the interfacial tension is $\gamma = 4.2 \pm 0.3$ mN/m. The emulsified drop preserves this shape until its final freezing at 14 °C. These results clearly show that the deformation of the emulsified drops does not require ultralow interfacial tension γ (<0.1 mN/m) as suggested in ref 2.

We performed similar experiments with surfactant $C_{18}\text{SorbEO}_{20}$, which induces drop-shape transformations starting at T_d around the bulk oil melting temperature, $T_d \approx T_m$ (belongs to Group B in the classification from ref 4). As seen in Figure 3, the deformation of the emulsified drops in this system starts at temperature $T_d = 18.5 \pm 0.5$ °C when the interfacial tension is $\gamma = 7.3 \pm 0.2$ mN/m. The emulsified drop acquires the shape of a planar platelet in the temperature range

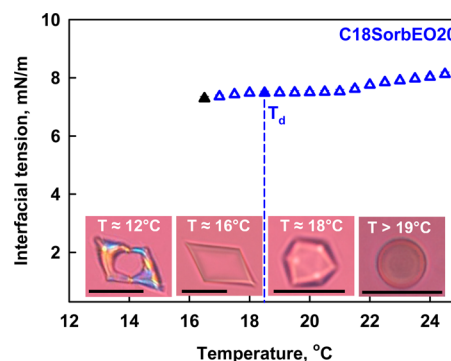


Figure 3. Interfacial tension as a function of temperature, as measured by the pendant drop method, for a hexadecane drop immersed in a 1.5 wt % (13.5 mM) aqueous solution of nonionic surfactant $C_{18}\text{SorbEO}_{20}$. The insets show microscope images of deformed drops captured at different temperatures. Note that the drop deformation starts at $T_d = 18.5 \pm 0.5$ °C when the interfacial tension is 7.3 ± 0.2 mN/m. The 1 mm pendant drop freezes at 16.5 ± 0.5 °C when the interfacial tension is still >7 mN/m, and the emulsified drop has a platelet shape at this temperature. Scale bars are $20 \mu\text{m}$.

of 16 to 17 °C when the interfacial tension is still higher than $\gamma = 7$ mN/m.

Next, we performed similar experiments with the system studied in ref 2—hexadecane drops in a 0.5 mM aqueous solution of $C_{18}\text{TAB}$ surfactant. This concentration of $C_{18}\text{TAB}$ falls in the range for this surfactant studied in ref 2 (between 0.3 and 1 mM). The results shown in Figure 4 demonstrate that

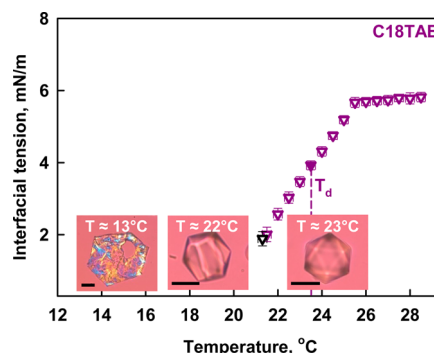


Figure 4. Interfacial tension as a function of temperature, measured by the pendant drop method, for a hexadecane drop immersed in a 0.5 mM aqueous solution of cationic surfactant $C_{18}\text{TAB}$. The insets show microscope images of deformed drops captured at different temperatures. Note that the drop deformation starts at $T_d = 23 \pm 0.5$ °C when the interfacial tension is 4.0 ± 0.2 mN/m. The last measurement with the 1 mm pendant drop is at 21 °C when the interfacial tension γ is still 2 ± 0.3 mN/m, and the emulsified drop has the shape of a flattened platelet at this temperature. Scale bars are $20 \mu\text{m}$.

the drop deformation starts at temperature $T_d = 23 \pm 0.5$ °C when the interfacial tension is 4.0 ± 0.5 mN/m. The emulsified drop acquires the shape of a planar platelet in the temperature range of 21 to 22 °C when the interfacial tension is around 2 mN/m. From the comparison of the results for the interfacial tension and the drop images shown in Figure 4, we can conclude that this surfactant also induces drop deformations at T_d higher than the melting temperature of the hexadecane, $T_d > T_m \approx 18$ °C (i.e., it belongs to Group A in our classification).

It is worth noting that we do not see a direct general relationship between the onset of microdrop deformation and

the change in the slope of the interfacial tension versus temperature that corresponds to the start of the surface phase transition for the millimeter-sized oil drops used in the pendant drop method^{2,3} (Figures 2–4). This lack of correlation indicates that the drop deformation most probably starts with the formation of local surface nuclei, without a complete prefreezing of the adsorption layer that would be detected by the pendant drop method. Furthermore, we may hypothesize that the formation of such surface nuclei and/or their further development into a bulk rotator phase should be easier for the smaller droplets, as evidenced by the fact that the large millimeter-sized pendant drops do not deform at the temperatures at which the micrometer droplets have evolved deep into the self-shaping phenomenon. The role of drop-surface curvature for surface nucleation, rotator phase formation, and related drop-shape transformations in these systems is discussed in detail in section 4 of ref 4.

All of these results convincingly demonstrate that the deformation of the emulsified drops does not require ultralow interfacial tension γ (<0.1 mN/m) and in all of the systems reported so far transformations start at $\gamma > 4.0 \pm 0.2$ mN/m. This result has a very important consequence because it sets a lower limit for the bending moment that is needed to deform the oil–water interface in these systems. As explained in ref 1, one needs a bending moment that is sufficiently high to counterbalance the capillary pressure of the curved drop surface (eq 2):

$$K_B/r^3 \geq \gamma/r \quad (2)$$

Here, K_B is the bending elasticity constant, r is the characteristic radius of curvature of the deformed drops, K_B/r^3 is an approximate estimate of the bending moment that drives the drop-surface deformation, and γ/r is the capillary pressure that opposes drop-surface deformation. Taking the typical values of $\gamma \approx 5$ mN/m and $r \approx 1$ μm , one estimates for the bending elasticity constant $K_B \geq \gamma r^2 \approx 5 \times 10^{-15}$ J. The latter value is 3 to 4 orders of magnitude higher than the bending moment of frozen surfactant or lipid monolayers and bilayers, $K_B \approx 10^{-18}$ to 10^{-17} J.^{2,21,22} Therefore, one cannot explain the observed drop deformations with the bending moment of the frozen surfactant monolayers or bilayers.

As explained in ref 1, a sufficiently high bending moment could be created by a subsurface multilayer of self-assembled alkane molecules. This explanation is supported by the experimental fact^{8–10} that the hexadecane drops may undergo a phase transition from liquid into so-called plastic phases around the melting temperature of hexadecane, $T_m \approx 18$ °C. These plastic phases are a kind of smectic phase (lamellar multilayers) with long-range translational order of the incorporated molecules (Figure 5). They are called also rotator

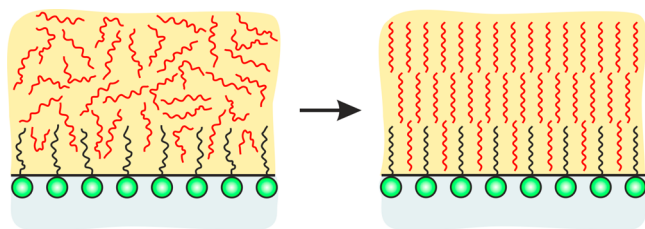


Figure 5. Schematic presentation of the mechanism of formation of a rotator-phase multilayer, templated by a frozen surfactant adsorption layer.^{1,4}

phases in the literature because the alkane molecules in these phases are not completely frozen and have rotational mobility around their long axes.^{5,6,23} These plastic phases appear as intermediate stable or metastable phases between the isotropic liquid phase, observed at temperatures above T_m , and the completely frozen solid phase, observed at lower temperatures. Typically, the temperature range of the appearance of the plastic rotator phases is from several degrees above T_m down to several degrees below T_m . Furthermore, these plastic rotator phases were observed in hexadecane drops only when the latter were dispersed in solutions of long-tail surfactants (C_{16} or C_{18}), the same as the surfactants that drive the observed drop-shape transformations.^{1,4,8}

The numerical estimates show¹ that a thin plastic sheet of ordered alkane molecules, templated by the surfactant adsorption layer and having a thickness of $h_{PL} \approx$ several hundred nanometers, may have a sufficiently high bending moment to explain the observed experimental results. These estimates are based on the fact that K_B is proportional to h_{PL}^2 for phases with a long-range molecular order, as it is the case with the plastic phases.²² On the other hand, there is an upper limit for the thickness of such potential stiff layers placed by the curvature of the edges of the platelets and of the threads protruding from their corners, both being observed to have a radius of <3 μm .

Let us note that the other arguments, used by Guttman et al.^{2,3} to support their mechanism, also suffer from serious deficiencies. For example, these authors used the expression^{2,3}

$$\frac{d\gamma}{dT} = -S_I \quad (3)$$

to interpret their data for the change in interfacial tension with temperature in order to prove that only an adsorption monolayer is frozen on the interface and no plastic phase multilayer has been formed. Here, γ is the interfacial tension, T is the temperature, and S_I is the excess of surface entropy, viz., the excess entropy of molecules in the surface layer as compared to that of molecules in the bulk phases. In fact, eq 3 is valid for a one-component system only, i.e., for the interface between a one-component liquid phase and a vacuum or gas phase containing vapors of the same liquid. This equation cannot be applied to the emulsions considered in our studies^{1–4} because the complete equation for an oil–water interface in the presence of surfactant molecules has two additional terms:²⁴

$$\frac{d\gamma}{dT} = -S_I - \frac{\Gamma_S d\mu_s}{dT} - \frac{\Gamma_A d\mu_A}{dT} \quad (4)$$

Here, Γ_S and Γ_A are the adsorptions of surfactant and alkane, respectively, and μ_s and μ_A are their chemical potentials. This equation is strictly valid for a tricomponent system in equilibrium (water, alkane, surfactant) with a planar alkane–water interface and a dividing surface chosen to coincide with the so-called equimolecular surface of water, at which water adsorption is identically zero.²⁴ The complete analysis of the experimental data by eq 4 is beyond the scope of the present study because other effects could be important, e.g., the effects of interfacial curvature or the temperature dependence of the chemical potential $\mu_{s(0)}$ of the surfactant dissolved in the aqueous phase, and would require additional terms to be included.²⁴ However, even just the terms in eq 4 are sufficient to demonstrate that the arguments by Guttman et al.^{2,3} are (at least) incomplete because the term $\Gamma_S d\mu_s/dT \approx -\Gamma_S k_B \ln x_s \approx 10\Gamma_S k_B \approx +0.5 \times 10^{-3}$ J m⁻² K⁻¹, omitted by these authors, is

comparable in magnitude and opposite in sign to the excess interfacial entropy, $S_1 \approx -0.9 \times 10^{-3} \text{ J m}^{-2} \text{ K}^{-1}$, considered in refs 2 and 3. Here, k_B is the Boltzmann constant and x_s is the mole fraction of surfactant in the aqueous solution. In this estimate, we have assumed an ideal surfactant solution with adsorption $\Gamma_s \approx 5 \mu\text{mol/m}^2$. Although the latter assumptions might not be perfectly valid, slight deviations from the values assumed would not change the order-of-magnitude estimate of the additional term in eq 4, related to surfactant adsorption, so it should not be ignored. Until the opposite is proven, similarly there are no reasons to expect that the other term in eq 4, related to the adsorption of alkane molecules, could be neglected either or that it could counterbalance the term related to surfactant adsorption. The terms related to the changing curvature add further complexity to the thermodynamic analysis of the system.

We have reason to express concern about the measurements by Guttman et al.^{2,3} of the interfacial tension from the size of the wetting film formed between an oil drop and the glass wall of the container in which the emulsion droplets are enclosed. The equation used by Guttman et al.^{2,3} to interpret the respective experimental data is based on the balance of the buoyancy force (which pushes the drop upward) and the repulsive disjoining pressure (exactly equal to the capillary pressure of the drop, $2\gamma/R$) inside the film area, which creates a repulsive force and stops the drop from rising:

$$\frac{4}{3} \Delta \rho g \pi R^3 = \pi r_F \frac{2\gamma}{R} \Rightarrow \gamma = \frac{2}{3} \Delta \rho g \frac{R^4}{r_F^2} \quad (5)$$

Here, $\Delta \rho \approx 230 \text{ kg/m}^3$ is the difference in mass densities of the aqueous and hexadecane phases, g is the acceleration due to gravity, R is the radius of the spherical drop, and r_F is the radius of the planar wetting film. This equation is valid only in the absence of attractive interactions between the drop and the solid surface; otherwise, an additional attractive term appears to complete the force balance.^{25–27} In the experiments by Guttman et al.,^{2,3} however, the bare glass is negatively charged, whereas the drop surface is covered by an adsorption layer of positively charged surfactant molecules. In such systems, the film could have a much larger radius than the one predicted by eq 5 because the additional attractive force between the oppositely charged surfaces expands the contact area, as this is the energetically favored equilibrium configuration.²⁷ This interaction is the main reason for the use of cationic polymers and surfactants as flocculants for negatively charged particles.

To check how eq 5 describes our experimental data, we tried this method for hexadecane drops, dispersed in an aqueous solution of nonionic surfactant $C_{18}\text{SorbEO}_{20}$, at several temperatures, including 19°C , which is just at the onset of drop self-shaping transitions in this system. The nonionic surfactants are known to create steric and electrostatic repulsion between surfaces^{28,29} so that no attraction between the oil droplets and the glass surface appears in this system and eq 5 is valid. In Figure 6A, we show a micrograph image in reflected light of the contact zone between a hexadecane drop and a glass solid wall (the upper wall of the glass capillary, containing the emulsions in our experiments) exactly in the moment when the drop deformations start. One sees the central contact zone, appearing as a bright circular spot, and the Newton fringes around it that indicate the changes in the local thickness of the oil–water–glass wetting film in the contact zone. From the position of the fringes and the known

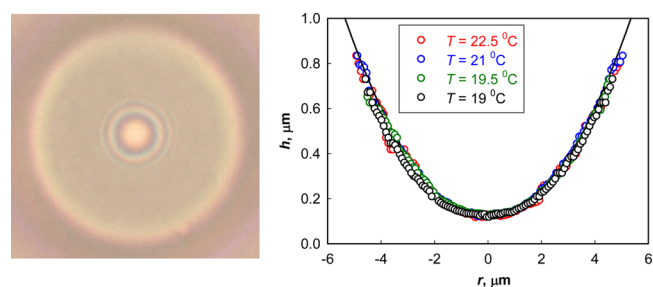


Figure 6. (Left) Micrograph image of the wetting film formed when a hexadecane drop, immersed in a 1.5 wt % $C_{18}\text{SorbEO}_{20}$ solution, is in contact with the glass surface of the capillary used for drop observations. Reflected light is used to detect the interference Newton rings in the contact zone, which can be used to restore the shape of the oil–water interface in the contact zone. This image is taken at 19.0°C , in the moment at which the first drop deformation events occur. (Right) Restored drop profiles in the contact zone, as determined at 22.5, 21, and 19.5°C . These profiles coincide with each other in the framework of the experimental accuracy, and no visible planar film could be detected. If there is a planar film, its diameter is below $1 \mu\text{m}$, which means that the drop interfacial tension is above 0.2 mN/m at all temperatures studied, including that of the drop-shape transition onset. For comparison, the black curve is a plot of a spherical surface with the measured drop diameter.

wavelength of light ($\lambda \approx 555 \text{ nm}$), one could restore the profile of the oil–water interface in the contact zone.³⁰ The profiles obtained at four of the temperatures studied (Figure 6B) show that the droplet has preserved a spherical shape, without any visible flattening in the contact zone, down to the temperature of the self-shaping transitions despite the presence of the bright area in the contact zone, seen in Figure 6A. In fact, the four profiles taken at 22.5, 21, 19.5, and 19°C coincide with each other in the framework of our experimental accuracy. Although the central bright zone could be mistaken for a planar wetting film, the restored profiles show that the drop is not deformed before the self-shaping process starts, which means that the drop interfacial tension is not ultralow at the onset of the shape transitions. From eq 5, one could estimate that the drop shown in Figure 6 has an interfacial tension of $\gamma > 0.2 \text{ mN/m}$ for all temperatures studied (in agreement with $\gamma \approx 8 \text{ mN/m}$ from our independent measurement, Figure 3); otherwise, the wetting film would be large enough to be detected with the optical resolution of the microscope used (ca. $1 \mu\text{m}$). Similar results were obtained with all of the other surfactants studied.

The other type of experiment, used by Guttman et al. to measure the interfacial tension, is also not convincing. The Wilhelmy plate method is appropriate and is widely used for measurements of the liquid–air interfacial tension because it requires perfect wetting of the Wilhelmy plate by the liquid. This wetting could be achieved for a liquid–air interface with special treatment of the plate surface or by using plates prepared from filter paper, but it is highly problematic for oil–water interfaces in the presence of cationic surfactants. Good wetting is expected to be a serious issue in the latter systems because the cationic surfactants are often used as hydrophobizing (opposite to wetting) agents.²¹ Therefore, the data from the Wilhelmy plate measurements, reported by Guttman et al.,^{2,3} also cannot be accepted without doubt, unless the authors prove that the Wilhelmy plate was perfectly wetted by the water phase in the entire range of measurements made by them.

Finally, for a surfactant monolayer to be able to bend the interface against the capillary pressure forces, the interfacial tension should be on the order of 10^{-3} mN/m or lower. Such low interfacial tensions could be measured with a very limited number of methods, e.g., by the spinning drop method. Unless such special methods for ultralow tensions are applied, the measurements could not give reliable results for such systems.

On the other hand, even the lowest interfacial tension measured in our systems at the onset of drop self-shaping, ~ 1 mN/m, would require a molecular multilayer, with a bending moment by a factor of at least 10^2 to 10^3 higher than the bending moment of the strongest monolayers known so far and used by Guttman et al.^{2,3} in their estimates to explain the self-shaping phenomenon. The plastic interfacial sheet of self-assembled alkane molecules, detected years ago by X-ray and DSC methods in such alkane droplets,^{8–11} consists of molecular structures that could certainly possess such a high bending moment and explain the drop self-shaping phenomenon.

CONCLUSIONS

The experimental results presented in the current study demonstrate unambiguously that the drop-shape transformations, observed in refs 1–4, do not require ultralow interfacial tension, as suggested in ref 2. Instead, these transformations typically start at temperatures at which the interfacial tensions are in the range of 4 to 8 mN/m.

As estimated in ref 1, the bending constant of a single surfactant monolayer or bilayer (on the order of 10^{-18} J) is far too weak to cause the observed drop-shape transformations.^{1–4} A bending constant on the order of 10^{-15} to 10^{-14} J is needed to effect this process. As explained in ref 1, this is possible for a multilayer of alkane molecules self-assembled into the so-called rotator phases.^{5,6,23} As a result of their long-range order, the rotator phases are rather stiff and are therefore often called plastic phases in the literature.^{6,23} We emphasize that such phases were experimentally detected in hexadecane drops^{8–11} under similar conditions (C_{16} – C_{18} surfactants at temperatures around the hexadecane melting temperature) well before the drop self-shaping phenomenon was discovered.¹

In conclusion, the presented results strongly support the mechanism described in ref 1.

ASSOCIATED CONTENT

Supporting Information

The Supporting Information is available free of charge on the ACS Publications website at DOI: 10.1021/acs.langmuir.6b01626.

Properties of surfactants studied. Interfacial tension of the pure hexadecane–water interface. Interfacial tension as a function of temperature for a hexadecane drop immersed in an aqueous solution of nonionic surfactant $C_{16}EO_{20}$. Interfacial tension as a function of temperature for a hexadecane drop immersed in an aqueous solution of nonionic surfactant $C_{16-18}EO_{50}$. (PDF)

AUTHOR INFORMATION

Corresponding Author

*E-mail: sks46@cam.ac.uk. Tel: (01223) 334435. Fax (01223) 762088.

Notes

The authors declare no competing financial interest.

ACKNOWLEDGMENTS

This work was funded by the European Research Council (ERC) grant to Stoyan Smoukov, EMATTER (# 280078). The study falls under the umbrella of European networks COST MP 1106 and 1305. The authors are especially grateful to Dr. Zahari Vinarov, Dr. Konstantin Golemanov and Mrs. Mila Temelska (Sofia University) for performing some of the measurements and for the useful discussions.

REFERENCES

- (1) Denkov, N.; Tcholakova, S.; Lesov, I.; Cholakova, D.; Smoukov, S. K. Self-shaping of oil droplets via the formation of intermediate rotator phases upon cooling. *Nature* **2015**, *528*, 392–395.
- (2) Guttman, S.; Sapir, Z.; Schultz, M.; Butenko, A.; Ocko, B.; Deutsch, M.; Sloutskin, E. How faceted liquid droplets grow tails. *Proc. Natl. Acad. Sci. U. S. A.* **2016**, *113*, 493–496.
- (3) Guttman, S.; Ocko, B.; Deutsch, M.; Sloutskin, E. From faceted vesicles to liquid icoshedra: Where topology and crystallography meet. *Curr. Opin. Colloid Interface Sci.* **2016**, *22*, 35–40.
- (4) Cholakova, D.; Denkov, N. D.; Tcholakova, S.; Lesov, I.; Smoukov, S. K. Control of drop shape transformations in cooled emulsions. *Adv. Colloid Interface Sci.* **2016**, DOI: 10.1016/j.cis.2016.06.002.
- (5) Sirota, E.; King, H.; Singer, D.; Shao, H. Rotator phases of the normal alkanes: An x-ray scattering study. *J. Chem. Phys.* **1993**, *98*, 5809–5824.
- (6) Sirota, E.; Herhold, A. Transient phase-induced nucleation. *Science* **1999**, *283*, 529–532.
- (7) Wu, X.; Ocko, B.; Sirota, E.; Sinha, S.; Deutsch, M.; Cao, B.; Kim, M. Surface tension measurements of surface freezing in liquid normal alkanes. *Science* **1993**, *261*, 1018–1021.
- (8) Shinohara, Y.; Takamizawa, T.; Ueno, S.; Sato, K.; Kobayashi, I.; Nakajima, M.; Amemiya, Y. Microbeam X-Ray diffraction analysis of interfacial heterogeneous nucleation in n-hexadecane inside oil-in-water emulsion droplets. *Cryst. Growth Des.* **2008**, *8*, 3123–3126.
- (9) Shinohara, Y.; Kawasaki, N.; Ueno, S.; Kobayashi, I.; Nakajima, M.; Amemiya, Y. Observation of the transient rotator phase of n-hexadecane in emulsified droplets with time-resolved two-dimensional small- and wide-angle X-Ray scattering. *Phys. Rev. Lett.* **2005**, *94*, 097801.
- (10) Ueno, S.; Hamada, Y.; Sato, K. Controlling polymorphic crystallization of n-alkane crystals in emulsion droplets through interfacial heterogeneous nucleation. *Cryst. Growth Des.* **2003**, *3*, 935–939.
- (11) Gulseren, I.; Coupland, J. N. Surface melting in alkane emulsion droplets as affected by surfactant type. *J. Am. Oil Chem. Soc.* **2008**, *85*, 413–419.
- (12) Kandori, K.; Gaonkar, A., Eds.; *Applications of Microporous Glass Membranes: Membrane Emulsification*; Elsevier: 1995; p 113.
- (13) Charcosset, C.; Limayem, I.; Fessi, H. The membrane emulsification process – a review. *J. Chem. Technol. Biotechnol.* **2004**, *79*, 209–218.
- (14) Christov, N.; Ganchev, D.; Vassileva, N.; Denkov, N.; Danov, K.; Kralchevsky, P. Capillary mechanisms in membrane emulsification: oil-in-water emulsions stabilized by Tween 20 and milk proteins. *Colloids Surf, A* **2002**, *209*, 83–104.
- (15) Nakashima, T.; Shimizu, M.; Kukizaki, M. Membrane emulsification by microporous glass. *Key Eng. Mater.* **1992**, *61–62*, 513–516.
- (16) Newton, R. H.; Haffegge, J. P.; Ho, M. H. Polarized light microscopy of weakly birefringent biological specimens. *J. Microsc.* **1995**, *180*, 127–130.
- (17) Holmberg, K. *Handbook of Applied Surface and Colloid Chemistry*; John Wiley & Sons: 2001; Chapter 16, Vol. 2, pp 299–332.
- (18) Rotenberg, Y.; Boruvka, L.; Neumann, A. W. Determination of surface tension and contact angle from shapes of axisymmetric fluid interfaces. *J. Colloid Interface Sci.* **1983**, *93*, 169–183.

- (19) Hoorfar, M.; Neumann, A. W. Recent progress in axisymmetric drop shape analysis (ADSA). *Adv. Colloid Interface Sci.* **2006**, *121*, 25–49.
- (20) Bird, R. B.; Stewart, W. E.; Lightfoot, E. N. *Transport Phenomena*, 2nd ed.; Wiley: New York, 2002; Example 12.1–2, pp 376–378.
- (21) Israelachvili, J. N. *Intermolecular and Surface Forces*. Academic Press: Burlington, MA, 2011.
- (22) Evans, E. A.; Skalak, R. *Mechanics and Thermodynamics of Biomembranes*. CRC Press: Boca Raton, FL, 1980.
- (23) Small, D. M. *The Physical Chemistry of Lipids: From Alkanes to Phospholipids*. Plenum Press: New York, 1986.
- (24) Rowlinson, J. S.; Widom, B. *Molecular Theory of Capillarity*; Clarendon Press: Oxford, U.K., 1982.
- (25) Kralchevsky, P. A.; Ivanov, I. B. On the Mechanical Equilibrium between a Film of Finite Thickness and the External Meniscus. *Chem. Phys. Lett.* **1985**, *121*, 111–116.
- (26) Kralchevsky, P. A.; Ivanov, I. B. The Transition Region between a Thin Film and the Capillary Meniscus. *Chem. Phys. Lett.* **1985**, *121*, 116–121.
- (27) Denkov, N. D.; Petsev, D. N.; Danov, K. D. Flocculation of Deformable Emulsion Droplets. I. Droplet Shape and Line Tension Effects. *J. Colloid Interface Sci.* **1995**, *176*, 189–200.
- (28) Marinova, K. G.; Alargova, R. G.; Denkov, N. D.; Velev, O. D.; Petsev, D. N.; Ivanov, I. B.; Borwankar, R. P. Charging of Oil-Water Interfaces Due to Spontaneous Adsorption of Hydroxyl Ions. *Langmuir* **1996**, *12*, 2045–2051.
- (29) Marinova, K. G.; Denkov, N. D. Foam Destruction by Solid-Liquid Antifoams in Solutions of a Nonionic Surfactant: Electrostatic Interactions and Dynamic Effects. *Langmuir* **2001**, *17*, 2426–2436.
- (30) Born, M.; Wolf, E. *Principles of Optics*, 6th ed.; Elsevier Ltd.: 1980.